Smart Structures and Systems, *Vol. 25, No. 4* (*2020*) *459-469*
DOI: https://doi.org/10.12989/sss.2020.25.4.459

Cracked rotor diagnosis by means of frequency spectrum and artificial neural networks

B. Muñoz-Abella*, A. Ruiz-Fuentes [a], P. Rubio [b], L. Montero [c] and L. Rubio [d]

Department of Mechanical Engineering, *University Carlos III of Madrid*, *Av. de la Universidad*, *30*, *28911*, *Leganés*, *Madrid*, *Spain*

(*Received May 23, 2019, Revised July 24, 2019, Accepted August 12, 2019*)

Abstract. The presence of cracks in mechanical components is a very important problem that, if it is not detected on time, can lead to high economic costs and serious personal injuries. This work presents a methodology focused on identifying cracks in unbalanced rotors, which are some of the most frequent mechanical elements in industry. The proposed method is based on Artificial Neural Networks that give a solution to the presented inverse problem. They allow to estimate unknown crack parameters, specifically, the crack depth and the eccentricity angle, depending on the dynamic behavior of the rotor. The necessary data to train the developed Artificial Neural Network have been obtained from the frequency spectrum of the displacements of the well- known cracked Jeffcott rotor model, which takes into account the crack breathing mechanism during a shaft rotation. The proposed method is applicable to any rotating machine and it could contribute to establish adequate maintenance plans.

Keywords: rotor diagnosis; neural networks; crack identification; breathing mechanism; frequency spectrum

1. Introduction

Rotor systems play a fundamental role in many industrial applications since they are part of important mechanical components such as turbines, compressors, pumps and others. Specifically, one of the main elements of a rotor system is the rotating shaft. These parts can present multiple faults, such as misalignment, unbalance or transverse cracks. Fatigue cracks grow due to the action of bending and torsion cyclic stresses, which can originate a catastrophic failure that leads to personal injuries or high economic losses. So, it is needed to establish adequate maintenance plans in order to detect and identify the defect before it provokes an irreversible failure. The presence of defects in any mechanical component produces changes in its behavior, it causes a decrease of the stiffness that originates an increase of the displacements, a decrease of the natural frequencies and modifications in the mode shapes. These changes can be used to detect and identify damages in the mechanical element by means of the inverse problem resolution, for example Civera *et al*. (2017), Liang *et al*. (2019) and Xu *et al*. (2019). In the case of cracked shafts belonging to rotor systems (Dong *et al*. 2004, Sekhar 2004, Babu *et al*. 2008, Zhang *et al*. 2013, Mohammed *et al*. 2014, Guo *et al*. 2017).

First of all, previous to the inverse problem, it is necessary to establish the direct problem. That is to say, to determine the dynamic behavior of the cracked rotor system in function of the crack parameters. In the literature one can find different models that are used to analyze the rotor systems. However, the most used one is a simplified model called "Jeffcott rotor model", that allows to know the dynamic behavior of unbalanced rotors (Dimarogonas 1992, Nelson 1998, Genta 2005). In the case of cracked rotors, to model the crack it is also necessary to take into account its state during the shaft rotation. In this sense, some authors use the simplest model that considers that the crack remains always open (Papadopoulos and Dimarogonas 1987, Papadopoulos 2008), other ones propose a model which supposes that, during the rotation, the crack is completely open or completely closed, switching crack model, (Muller *et al*. 1994, Pu *et al*. 2002, Qin *et al*. 2003, Gasch 2008) and, finally, the most complicated and realistic crack model is called "breathing crack model" and it considers that the crack opens and closes gradually during the shaft rotation, as a result of it, the behavior of the shaft becomes nonlinear (Jun *et al*. 1992, Darpe *et al*. 2004, Papadopoulos 2004, Patel and Darpe 2008, Rubio and Fernández-Sáez 2012).

When a shaft is rotating the geometric center of each section describes a path called orbit. That is the representation of two perpendicular transversal displace-ments of that point along the time. The shape and size of the orbits can give very good information about the existence and severity of the defect (Chan and Lai 1995, Sinou and Lees 2005, Al-Shudeifat and Butcher 2011, El Arem and Zid 2017, Guo *et al*. 2017). It is well known that orbits of ideal rotors, without any damage, are circular, while elliptical shapes correspond to unbalanced rotors. On the other hand, in the case of both cracked and unbalanced shafts, orbits remain elliptical out of critical or subcritical speeds, but if the rotor passes through one of them the orbit shape changes. In the

*Corresponding author, Associate Professor,
E-mail: mmunoz@ing.uc3m.es
[a] Ph.D. Student, E-mail: anruizf@ing.uc3m.es
[b] Associate Professor, E-mail: prubio@ing.uc3m.es
[c] Ph.D., E-mail: lamonter@ing.uc3m.es
[d] Professor, E-mail: lrubio@ing.uc3m.es

ISSN: 1738-1584 (Print), 1738-1991 (Online)

vicinity of rotation subcritical speeds such as $\frac{1}{2}\omega_c$, $\frac{1}{3}\omega_c$ or $\frac{1}{4}\omega_c$, where ω_c is the system critical speed, resonances appear and the orbits present a series a loops according the speed rotation. In general, it can be said that if the rotation speed is closed to $\frac{1}{n}\omega_c$ the number of internal loops in the orbit is n-1. Thus, the presence of loops in a shaft orbit can be an indicator of the existence of a crack (Guo *et al*. 2017, El Arem and Zid 2017, Al-Shudeifat and Butcher 2011).

In the same way, the frequency spectrum obtained from the orbit displacements signal can lead, when the inverse problem is approached, to effective diagnosis of rotating system since its appearance depends on the type of damage. In the case of a cracked unbalanced rotor, the frequency spectrum presents, at any speed, two peaks. The first one appears at the speed rotation (called superharmonic $1X$) and it is due to the unbalance, and the second one can be found at twice the rotation speed (called superharmonic $2X$) and it is because of the crack (Darpe *et al*. 2004, Sinou 2008, Varney and Green 2013, El Arem and Zid 2017, Ansari *et al*. 2017). Besides, if the rotation of speed is close to a subcritical speed $\frac{1}{n}\omega_c$, as explained before, resonances appear and the frequency spectrum presents an additional peak that is located at n times the rotation speed (called superharmonic nX). Finally, it is necessary to take into account, according to Sinou (2008), the importance of the crack-unbalance interaction since it can modify both $1X$ vibration amplitude and nX subcritical resonant peaks.

Once the direct problem is known, the inverse problem must be approached. The simplest issue consists only in detecting if there is or not a defect, but the most complex one, usually called identification, it is related to determine the location or /and the characteristics of the crack. Various techniques have been proposed to detect faults in rotors, as you can find in the reviews (Sabnavis *et el*. 2004, Kumar and Rastogi 2009, Walker *et al*. 2013, Mogal and Lalwani 2014, Chandra and Sekhar 2016). One of the most used technique to achieve this purpose is to analyze the vibratory behavior of the rotor system. Some authors study the variation of the first rotor critical speed as a function of the crack depth at various rotation speeds (Chan and Lai 1995, Sinou and Lees 2005, 2007, Xiang *et al*. 2008, Al-Shudeifat and Butcher 2011, Ansari *et al*. 2017), the first critical speed decreases because of the stiffness decrease originated by the crack, besides the critical speed values decrease when the size crack increases. It can also be found works about the relationship between the crack depth and the frequency spectrum of the rotor, the peaks amplitude that appear at the vicinity of critical speeds increase when the damage depth grows and the closer the rotation speed is to the subharmonics the greater the amplitude is (Darpe *et al*. 2004, Sekhar 2004, Sinou 2008, Gasch 2008, Al-Shudeifat and Butcher 2010, Guo *et al*. 2013, 2017, Varney and Green 2013, Cavalini *et al*. 2016). Regarding the unbalance effects on the vibratory behavior, depending on the relative angle between the unbalance force and the perpendicular direction to the crack front, it can modify the vibrational response and mask the crack due to 1X component amplitude can increase or decrease and the other nX amplitudes can also change, besides it must take into account that in most cases this angle is unknown (Gómez-Mancilla *et al*. 2004, Darpe *et al*. 2004, Sinou 2008, Spagnol *et al*. 2018).

Furthermore, in order to establish maintenance plans, it is necessary to identify and not only detect the rotor faults. To achieve this target, some authors approach the inverse problem by means of different techniques, Sekhar (2004) obtains the crack parameters by using the Least Square fitting considering that the crack effects are produced by external virtual forces, Söffker *et al*. (2016) take into account virtual forces too, nevertheless Proportional Integral Observer (PIO) technique is used to detect the damage. On the other hand, correlation filtering and Laplace wavelet is used by Dong *et al*. (2009) to estimate the modal parameters, Sampaio and Nicoletti (2016) detect the crack by the Approximated Entropy Algorithm from the rotor vertical displacement and Xiang *et al*. (2008) apply the Genetic Algorithms technique to the data obtained from the system vibratory behavior. Lastly, there are various publications that use the Artificial Neural Networks (ANN) to determine some parameters related to the crack properties from the rotor full spectrum data (Adewusi and Al-Bedoor 2002, Abarici and Bilgin 2009).

ANN have widely been used in mechanical engineering because they are a very useful technique for a wide range of applications, such as classification, pattern recognition, optimization or prediction, even in the case of complex nonlinear problems (Liu *et al*. 2002, Muñoz-Abella *et al*. 2015, Hakim and Abdul Razak 2014, Civera *et al*. 2017, Park *et al*. 2018, Rubio *et al*. 2018, Kumar *et al*. 2018). Regarding the problem of damage identification and detection in rotors it can be found diverse works that apply ANN to face this question, among others, Wang and Chen (2009) and Abarici and Bilgin (2009) discriminate fault types for rotor systems by ANN, Adewusi and Al-Bedoor (2002) propose a novel method for machine health monitoring that uses ANN to detect both the propagating and no propagating cracks, Mohammed *et al*. (2014) apply 3 independent Neural Networks to identify patterns corresponding to different cracked shaft states, Kekan and Kumar (2019) identify a crack in a rotating shaft by means of Neural Networks and natural frequencies and Zapico-Valle *et al*. (2014) estimate both position and depth for a notch in a rotor.

In this paper, a new method for diagnosis of cracked and unbalanced rotor systems, that considers the breathing mechanism during the cracked shaft rotation, is presented. The proposed methodology, that is generalizable for any rotating machine, consists in approaching the inverse problem by means of a system formed by 2 Artificial Neural Networks, taking as input data the frequency spectrum of the cracked rotor and obtaining as output 2 unknown parameters, the crack size and the eccentricity angle. The methodology could contribute to establish adequate maintenance plans.

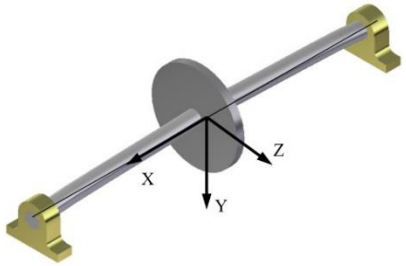

Fig. 1 Scheme of the cracked Jeffcott rotor model

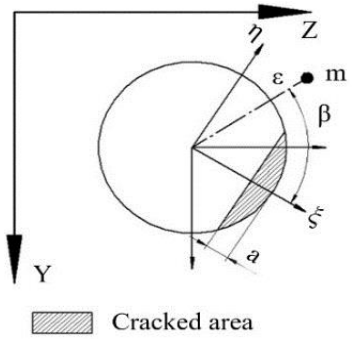

Fig. 2 Cracked section with both fixed and rotary coordinate systems

2. Direct problem. Jeffcott rotor model

The direct problem is the necessary first step to obtain the data to train the ANN. In this case, the rotor dynamic response will be obtained, specifically its frequency spectrum, in function of the crack depth and the eccentricity angle. The behavior of the rotor has been analyzed by means of a classical Jeffcott rotor model with a transverse crack. It consists of a massless shaft, of diameter D and lenght L, mounted on rigid supports with a disc of mass m at its mid-span (see Fig. 1).

The transverse crack, with straight front and depth a, is placed at the mid-span of the rotor. Besides, the rotor has an unbalance eccentricity ε, oriented an angle β measured with respect to the perpendicular direction to the crack front, as it can be seen in Fig. 2.

The equations of the motion for the geometric center of the cracked rotor in a fixed coordinate system (X, Y, Z) (Fig. 1) can be written

Table 1 Constant parameters of the chosen cracked rotor

L (m)	D (m)	E (GPa)	e	m (kg)	x
0.9	0.02	72	2.084	5.2	0.001

$$\begin{aligned} mY'' + cY' + k_{yy}Z + k_{yz}Z &= m\varepsilon\Omega^2\cos(\Omega t+\beta) + mg \\ mZ'' + cZ' + k_{yz}Y + +k_{zz}Z &= m\varepsilon\Omega^2\sin(\Omega t+\beta) \end{aligned} \quad (1)$$

where (*)' indicates time derivatives and Ω is the constant rotating speed of the shaft, c is the damping coefficient, meanwhile k_{yy}, k_{zz} and k_{yz} represent the stiffness coefficients.

According to the procedure presented by Rubio and Fernández Sáez (2012), Eq. (1) is integrated considering the stiffness coefficients in the rotational frame x-η. The motion equation, Eq. (1), can be written in non-dimensional form according to

$$\begin{aligned} &\ddot{\bar{Y}} + 2\xi\frac{1}{p}\dot{\bar{Y}} + \left(\frac{1}{p}\right)^2\overline{k_{yy}}\bar{Y} + \left(\frac{1}{p}\right)^2\overline{k_{yz}}\bar{Z} \\ &= e\cos(\tau+\beta) + \left(\frac{1}{p}\right)^2 \\ &\ddot{\bar{Z}} + 2\xi\frac{1}{p}\dot{\bar{Z}} + \left(\frac{1}{p}\right)^2\overline{k_{yz}}\bar{Y} + \left(\frac{1}{p}\right)^2\overline{k_{zz}}\bar{Z} = e\sin(\tau+\beta) \end{aligned} \quad (2)$$

where $(\dot{*})$ indicates derivative with respect to dimensionless time, τ. Employing the following dimensionless parameters

$$\bar{Y} = \frac{Y}{\delta_{st}}; \quad \bar{Z} = \frac{Z}{\delta_{st}}; \quad \tau = \Omega t; \quad \xi = \frac{c}{2\sqrt{k_o m}};$$
$$e = \frac{\varepsilon}{\delta_{st}}; \quad \overline{k_{yy}} = \frac{k_{yy}}{k_o}; \quad \overline{k_{yz}} = \frac{k_{yz}}{k_o}; \quad \overline{k_{zz}} = \frac{k_{zz}}{k_o}$$

Being t the time, δ_{st} the rotor static displacement due to the weight of the mass, k_o the stiffness of the uncracked rotor. Besides, p, the non-dimensional speed rotation, and α, the non-dimensional crack depth, are defined, respectively, s $p = \Omega/\omega_o$ and $\alpha = a/D$. Where ω_o is the natural frequency of the healthy system.

Some of the previous variables have been remained constant through the present study. They are shown in Table 1.

The calculation of $\bar{Y}$ and $\bar{Z}$ over the time has been done according to the procedure developed by Rubio and

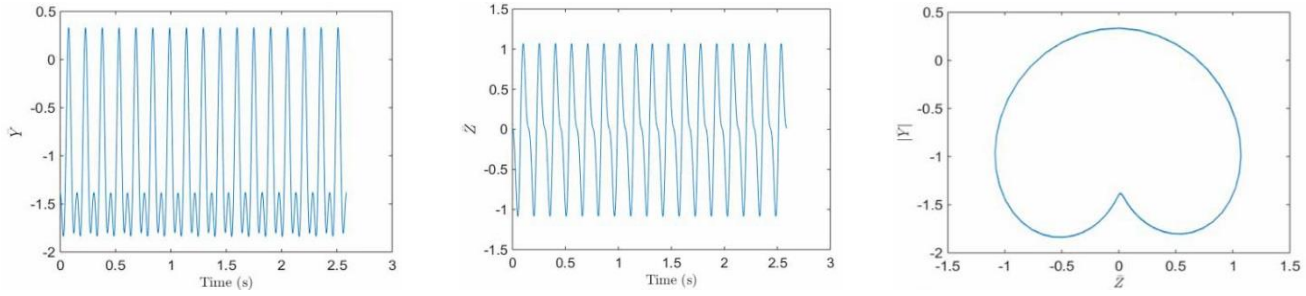

(a) $\bar{Y}$ over the time (b) $\bar{Z}$ over the time (c) Orbit of the geometric center of the rotor

Fig. 3 Example of the results from the Jeffcott rotor model (α = 0.48 and p = 0.49)

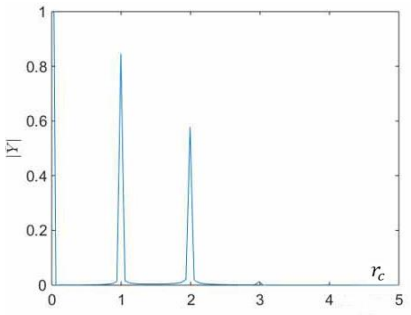

(a) $\overline{Y}$ frequency spectrum (FFT)

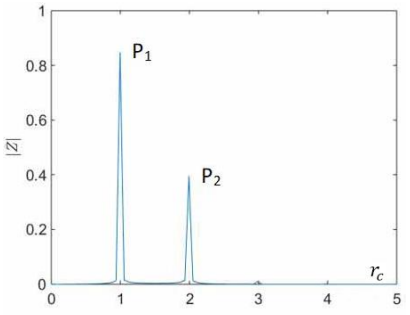

(b) $\overline{Z}$ frequency spectrum (FFT)

Fig. 4 Example of the FFT results from the Jeffcott rotor model, α = 0.48 and p = 0.49

Fernández Sáez (2012), which takes into account the crack breathing mechanism. Fig. 3 shows an example of the results that can be obtained from the Eq. (2). Figs. 3(a)-(b) show, respectively, the non-dimensional variables $\overline{Y}$ and $\overline{Z}$ in function of the time, as an example for the case of α = 0.48 and p = 0.49. In addition, in Fig. 3(c) it can be seen the described path by the geometric center of the cracked rotor, that it to say, its orbit.

From the original data $\overline{Y}$ and $\overline{Z}$ one can obtain the frequency spectrum by application of the Fast Fourier Transform (FFT). In Fig. 4 the spectrum from the Figs. 3(a) and (b) data, are shown.

The abscissa axis in Fig. 4 shows the non-dimensional speed $r_c = \frac{\omega_c}{\Omega}$, being ω_c the natural frequency of the cracked system.

The rotor used in this work presents two characteristics that always affect the number and amplitude of the frequency spectrum peaks, regardless of its speed. The first of them is the unbalanced mass that originates one peak at the rotating speed $r_c = 1$ in Fig. 4. The second one is the crack, which produces two peaks, one at the rotating speed and another at twice that speed, $r_c = 1$ and $r_c = 2$, respectively, in Fig. 4. In the next section, these two peaks corresponding to $\overline{Z}$, Fig. 4(b), have been chosen to perform the inverse problem through Artificial Neural Networks. They are called P_1 and P_2, respectively, (see Fig. 4(b)).

In order to get the required data for the ANN training in the inverse problem, different cases of crack depth, eccentricity angle and rotation speed have been considered, according to the following:

- Eight relative depths, varying from α = 0.1 until α = 0.45 in increments of 0.05.
- Fifty dimensionless rotation speeds, from p = 0.01 until p = 0.5 in increments of 0.01.
- Thirty-seven eccentricity angles, from β=0° until β = 180° in increments of 5°.

3. Inverse problem. Artificial Neural Network approach

An Artificial Neural Network is a flexible and robust mathematical tool that allows, among many other purposes, to establish nonlinear regression models, as in the case of

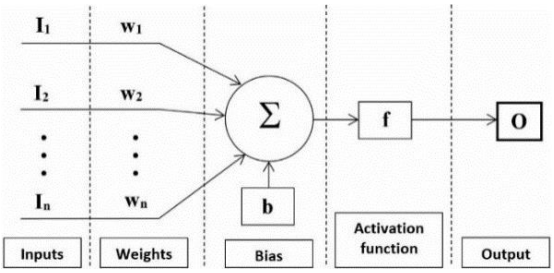

Fig. 5 Calculation scheme of a single neuron

a cracked rotor dynamics with breathing mechanism. An ANN is made up of a large number of basic processing units called neurons, that mimic the biological neurons and, like them, they are interconnected. Individually, a single neuron can accept several inputs (I_i) from other neurons or external sources, it performs modifications on the inputs and then passes the transformed information to other neurons or to the final output (O). Fig. 5 shows the calculation scheme into a single neuron. As can be seen, the neuron adds every input (I_i) weighted by the value (w_i) plus a threshold parameter called bias (b) and, finally, the sum goes through an activation function (f) which limits the value of the neuron output (O).

From among all the types of ANNs that exist, in this work the multilayer perceptron (MLP) feed forward neural network, trained with a back-propagation learning algorithm, has been used. Here the neurons are grouped into 3 types of layers according to their positions, they are called input, hidden and output layers. The first one is composed of neurons connected with external data, the second ones process and propagate the information from the input to the output layers and, finally, the output layer offers the wanted results.

Regarding the learning algorithm, it is a supervised training that consists in processing the inputs and comparing the obtained outputs against the desired outputs, so both the inputs and the outputs have to be previously provided, from the results calculated by the direct problem. Then the differences are propagated back through the net and the system adjusts iteratively the weights until the error is below than a predetermined value. After every iteration, other different sets of inputs and outputs values are used in the ANN validation. Finally, to confirm the predictive capability of the net, new couples of inputs and outputs data

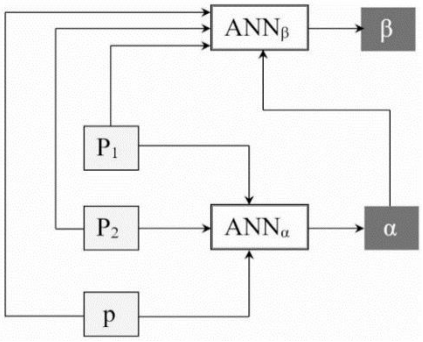

Fig. 6 Scheme of the proposed algorithm based on ANN

are used in the testing process.

In this work a methodology, based on the previous explained type of ANN, for identifying a crack in a rotor is presented. It consists in unbalancing the system in a controlled way, namely, a known eccentric mass is placed at an established distance from the center of the disc ε, according to Fig. 2. Then, the system is rotated under normal working conditions. Given a rotation speed, through a Neural Network approach it is possible to find a relationship between the FFT, obtained from the displacements of the center of the rotor, and the unknown searched crack properties (depth and orientation).

The developed method in this work consists of 2 MLP Neural Networks. One of them (ANN_α) allows to obtain the dimensionless crack size α and the second one (ANN_β) estimates the eccentricity angle β. In Fig. 6 the scheme of the proposed method is shown, where the ANN inputs and outputs can be found.

As it is shown in Fig. 6 the ANN_α inputs are the values of the peaks, P_1 and P_2, and the dimensionless rotation speed p, obtained from the Jeffcott rotor model, and the output is the crack depth ratio α. On the other hand, the value of α calculated by ANN_α is used as one of the ANN_β inputs, in addition to P_1, P_2 and p, while its output is the eccentricity angle β. Both networks are of type feed-forward Levenberg-Marquardt backpropagation and they have been implemented in MATLAB (Matlab 2002).

In order to achieve an adequate ANN training (better performance and faster convergence), it is usually necessary to transform the input data using an appropriate transformation method (Shanker *et al.* 1996). In this work, the values of the input variables are between 0 and 1, so the eccentricity angle β has been processing by

$$\beta' = \frac{\beta - \beta_{min}}{\beta_{max} - \beta_{min}} = \frac{\beta}{180^\circ} \tag{3}$$

where β' is the transformed eccentricity angle, and β_{max} and β_{min} are the maximum and minimum β values, respectively.

The available calculated data from the rotor analytical model have randomly been divided into 2 sets, one of them is composed of values used for the ANN training and the second one contains the data for the nets validation. Both, for ANN_α and for ANN_β, there are 13650 and 3000 data for training and validation, respectively. Regarding the activation functions (f), in all layers, log-sigmoidal function has been chosen since it is suggested to use non-linear activation functions in the case on non-linear data relationships (Haykin 1998).

Table 2 Study of the ANN_α architecture

	Training		Validation	
ANN architecture	R^2	MSE	R^2	MSE
[3 3 1]	0.9583	$1.4{\cdot}10^{-3}$	0.9582	$1.5{\cdot}10^{-3}$
[3 5 1]	0.9653	$1.2{\cdot}10^{-3}$	0.9588	$1.3{\cdot}10^{-3}$
[3 10 1]	0.9944	$18.6{\cdot}10^{-3}$	0.9943	$23.6{\cdot}10^{-3}$
[3 15 1]	0.9957	$15.3{\cdot}10^{-3}$	0.9942	$19.2{\cdot}10^{-3}$
[3 3 3 1]	0.9621	$1.2{\cdot}10^{-3}$	0.9611	$1.3{\cdot}10^{-3}$
[3 5 3 1]	0.9924	$2.5{\cdot}10^{-4}$	0.9921	$2.9{\cdot}10^{-4}$
[3 5 5 1]	0.9938	$2.26{\cdot}10^{-4}$	0.9901	$3.9{\cdot}10^{-4}$
[3 7 5 1]	0.9966	$1.22{\cdot}10^{-4}$	0.9958	$1.8{\cdot}10^{-4}$
[3 7 7 1]	**0.9975**	$\mathbf{8.7{\cdot}10^{-5}}$	**0.9965**	$\mathbf{1.63{\cdot}10^{-4}}$
[3 10 5 1]	0.9966	$1.39{\cdot}10^{-4}$	0.9947	$2.04{\cdot}10^{-4}$
[3 10 7 1]	0.9967	$1.29{\cdot}10^{-4}$	0.9952	$2.18{\cdot}10^{-4}$
[3 10 10 1]	0.9983	$6{\cdot}10^{-5}$	0.9977	$1.27{\cdot}10^{-4}$

To choose the adequate number of layers and neurons for both nets, a study with different ANN architectures has been made. The variables used to check the accuracy of the neural networks estimations are R^2 and MSE, both during the training and validation steps. Being MSE the minimum mean squared error, according to Eq. (4).

$$MSE = Average[(X_{estimated} - X_{actual})^2] \quad \text{Being } X = \alpha,\ \beta \tag{4}$$

In the Table 2 one can see the obtained results for ANN_α. In the first column, the ANN structure is represented. Each figure represents a layer, and its value is the number of neurons for that layer.

Table 3 Study of the ANN_β architecture

	Training		Validation	
ANN architecture	R^2	MSE	R^2	MSE
[4 5 1]	0.8912	$1.8{\cdot}10^{-2}$	0.8892	$1.93{\cdot}10^{-2}$
[4 7 1]	0.9141	$1.46{\cdot}10^{-2}$	0.9116	$1.53{\cdot}10^{-2}$
[4 10 1]	0.9592	$7.2{\cdot}10^{-3}$	0.9557	$7.8{\cdot}10^{-3}$
[4 15 1]	0.9754	$4.3{\cdot}10^{-3}$	0.9759	$4.7{\cdot}10^{-3}$
[4 3 3 1]	0.9371	$1.11{\cdot}10^{-2}$	0.9311	$1.15{\cdot}10^{-2}$
[4 5 3 1]	0.9474	$9.2{\cdot}10^{-3}$	0.9433	$1{\cdot}10^{-2}$
[4 5 5 1]	0.9804	$3.5{\cdot}10^{-3}$	0.9787	$3.6{\cdot}10^{-3}$
[4 7 5 1]	0.9834	$3{\cdot}10^{-3}$	0.9819	$3.2{\cdot}10^{-3}$
[4 7 7 1]	0.9907	$1.6{\cdot}10^{-3}$	0.9903	$2.1{\cdot}10^{-3}$
[4 10 10 1]	0.9926	$1.4{\cdot}10^{-3}$	0.9897	$2.4{\cdot}10^{-3}$
[4 5 5 5 1]	0.9919	$1.4{\cdot}10^{-3}$	0.9913	$1.6{\cdot}10^{-3}$
[4 7 7 5 1]	0.9935	$1.2{\cdot}10^{-3}$	0.9915	$1.5{\cdot}10^{-3}$
[4 7 7 7 1]	**0.9959**	$\mathbf{8{\cdot}10^{-4}}$	**0.9943**	$\mathbf{1.8{\cdot}10^{-3}}$
[4 10 10 5 1]	0.9924	$6{\cdot}10^{-4}$	0.9898	$9{\cdot}10^{-4}$

According to Table 2 results, there are several nets that offer very good estimation values, since R^2 values are close to 1 and MSE results around $1 \cdot 10^{-4}$. Finally, it has been chosen the [3 7 7 1] architecture. It offers very good results, especially R^2 for the training step, with only 2 hidden layers and 7 neurons per layer.

In the same way, Table 3 shows the results of the analysis with different ANN architectures in the case of ANN_{β}.

Table 3 results show that in the case of ANN_{β} it is necessary more complex architectures than in the case of ANN_{α}, it can be because of there are 4 inputs instead of 3 and, besides, the relationship among inputs and output is more complex and highly non-linear. Finally, it has been chosen the [4 7 7 7 1] architecture that offers good results with the smallest possible number of neurons.

4. Verification of the proposed methodology

4.1 Comparison of real and predicted values

In order to verify the proposed method it is necessary to compare the estimated values by the ANN algorithm with the data obtained from the Jeffcott rotor analytical model. Two analysis have been done, first comparing ANN results with data used during the net training and, second, with data obtained from the analytical model that have not been used in the ANN design.

In addition, the final aim of the methodology it to apply it to real machines, so, to check the estimations goodness of the proposed method with actual data, random noise has been generated to mimic the real rotor systems and it has been added to the model numerical responses (specifically in p, P_1 and P_2 inputs) with 1%, 2% and 5% of its values as random noise.

4.1.1 Comparison with data used during the ANN training

Figs. 7-8 show the residuals of α, calculated as the difference between the analytical results from the Jeffcott rotor model (real) and the estimated data by the ANN, with respect to real α, for 7 different increasing β values (0°, 30°, 60°, 90°, 120°, 150° and 180°).

Two different situations have been considered. First, in Fig. 7 are shown the residuals corresponding to 3 rotation speeds, p = 0.1, p = 0.29 and p = 0.41, that have been chosen as an example of speeds which are not close to a rotor subcritical speed. Second, results corresponding to the vecinity of the critical speed submultiples, p = 0.25, p = 0.33 and p = 0.5, are shown in Fig. 8. The second cases can be considered critical situations since if the rotation speed is close to a subcritical speed. Then, the system can get a resonance frequency and becomes unstable.

It is necessary to say that in Figs. 7-10, axes limits have been chosen, depending on the case, in order to achieve the best view of the represented residuals.

Regarding crack size estimation, when the rotation speed is away from resonance speeds, see Fig. 7, the largest absolute discrepancies are always less than 0.015, independently from the value of the eccentricity angle orientation. However, if the rotation speed is equal or close to a subcritical speed, according to Fig. 8, the crack depth estimation is not so good when the speed is close to $\frac{1}{2}\omega_c$ (p = 0.5), in the worst case the α residual is around 0.15. However, for $\frac{1}{3}\omega_c$ (p = 0.33) the difference can be considered acceptable, less than 0.02, and for $\frac{1}{4}\omega_c$ (p = 0.25) the results are similar to the differences calculated in the case of being way from the resonances.

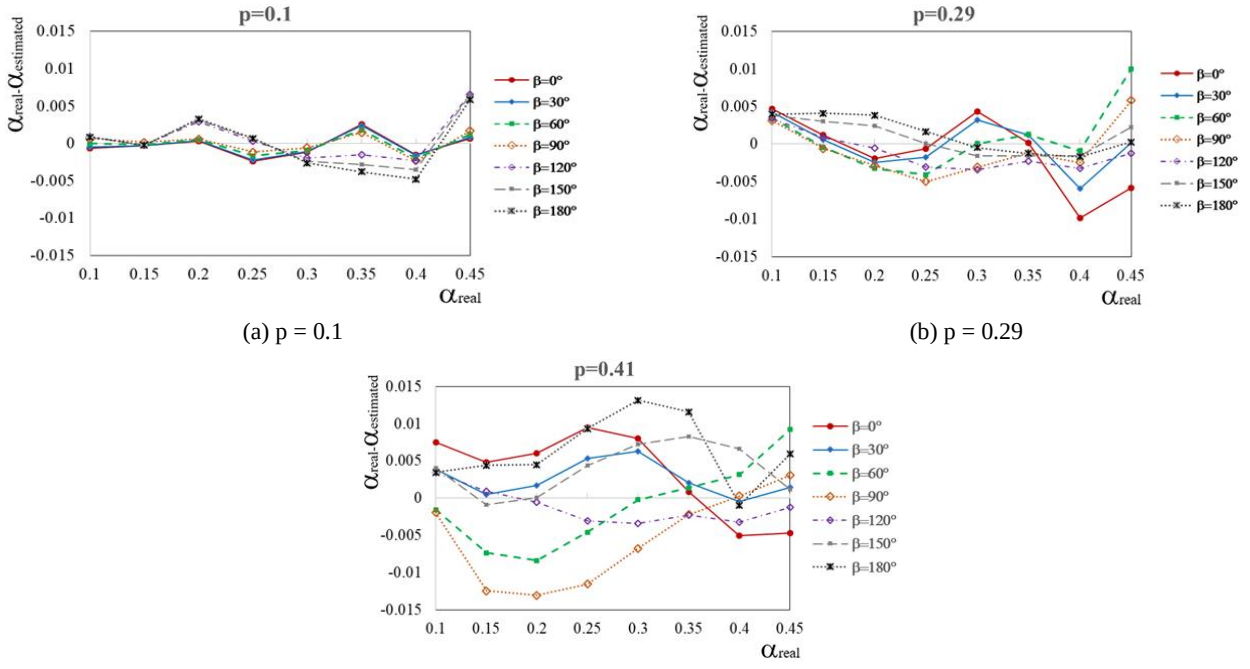

(a) p = 0.1

(b) p = 0.29

(c) p = 0.41

Fig. 7 Residuals of α for several β values. Rotation speeds are away from resonance speeds

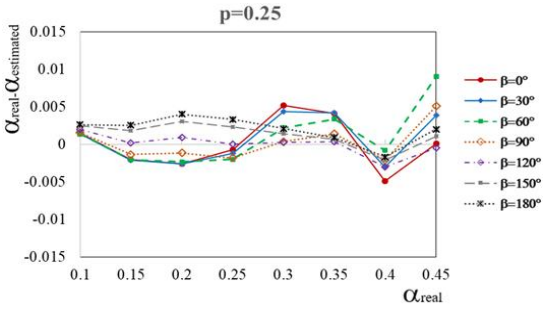

(a) p = 0.25

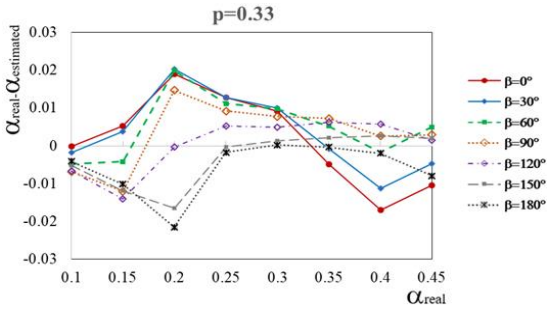

(b) p = 0.33

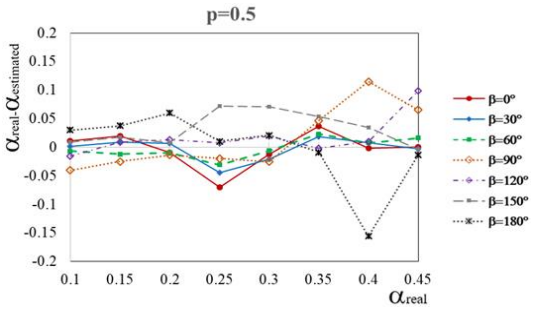

(c) p = 0.5

Fig. 8 Residuals of α for several β values. Rotation speeds are close to resonance speeds

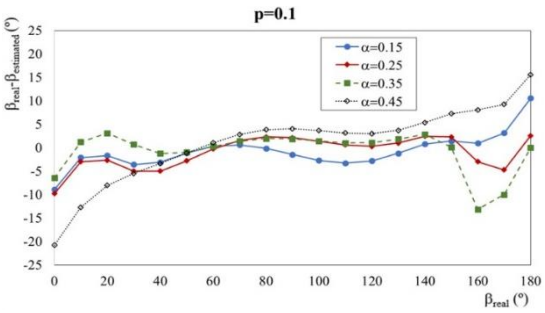

(a) p = 0.1

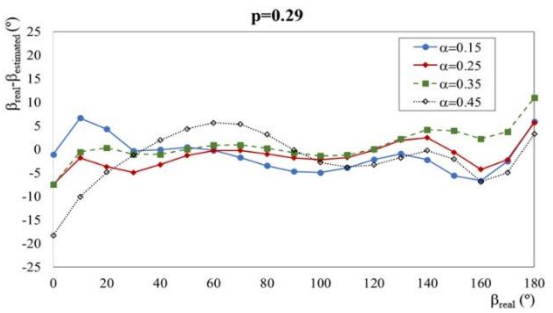

(b) p = 0.29

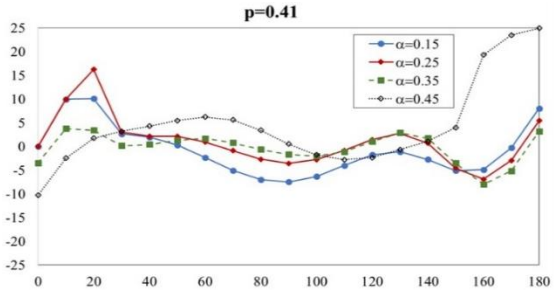

(c) p = 0.41

Fig. 9 Residuals of β for several α values. Rotation speeds are away from resonance speeds

In the same way, in order to study the β parameter effect, Figs. 9-10 show the residuals of β, calculated as the difference between the analytical results (real) and the estimated data by the ANN, with respect to the β real values, for 4 different increasing αvalues (0.15, 0.25, 0.35 and 0.45). Fig. 9 shows the β residuals for p = 0.1, p = 0.29 and p = 0.41, rotation speeds away from resonances, and Fig. 10 shows the β residuals for p = 0.25, p = 0.33 and p = 0.5, corresponding to critical speed submultiples.

In relation to β estimation, Figs. 9-10 show that the results obtained are also better for rotation speeds that are farther from the resonances, specially p = 0.33 and p = 0.5. For any speed away from the critical ones, the absolute discrepancies are between 1° and 10°, except if the eccentricity angle is close to the extreme values 0° or 180°. In these cases, they can reach until 25°. Among the analysed speeds, the best results are obtained for medium and low speeds.

Table 4 Residuals of α and β for input values different from the original ones (α = 0.18)

α	β (°)	p	α_{real} - $\alpha_{estimated}$	β_{real} (°) - $\beta_{estimated}$ (°)
		0.12	0.0007	7.78
	16	0.27	-0.0015	-4.53
		0.38	0.0038	13.98
		0.12	0.0008	-1.75
	38	0.27	-0.0020	-4.61
		0.38	0.0010	2.88
		0.12	0.0013	2.05
0.18	77	0.27	-0.0015	-1.88
		0.38	-0.0070	-2.80
		0.12	0.0019	-1.39
	113	0.27	0.0002	-2.81
		0.38	-0.0074	-2.02
		0.12	0.0024	9.49
	176	0.27	0.0040	3.51
		0.38	0.0038	9.05

Table 5 Residuals of α and β for input values different from the original ones (α = 0.31)

α	β (°)	p	α_{real} - $\alpha_{estimated}$	β_{real} (°) - $\beta_{estimated}$ (°)
		0.12	-0.0007	1.64
	16	0.27	0.0053	11.66
		0.38	-0.0021	-1.68
		0.12	-0.0008	-2.87
	38	0.27	0.0040	1.01
		0.38	-0.0022	-2.01
		0.12	-0.0009	0.94
0.31	77	0.27	0.0001	1.02
		0.38	-0.0045	-0.10
		0.12	-0.0009	-0.61
	113	0.27	-0.0017	-0.75
		0.38	0.0054	-4.21
		0.12	-0.0013	-2.47
	176	0.27	0.0002	4.11
		0.38	0.0080	0.85

4.1.2 Comparison with data used during the ANN training

In order to check the ANN goodness in the case of values that have not been used during its training, several data set (α, β and p) have randomly chosen, so that ANN algorithm estimations have been compared with the values obtained from the Jeffcott rotor model. According to the conclusions from the previous section, low and medium rotation speeds, different from resonances, have been preferred. Tables 4-6 show the residuals of α and β for 3 different α values, those are α = 0.18, α = 0.31 and α = 0.43.

Table 6 Residuals of α and β for input values different from the original ones (α = 0.43)

α	β (°)	p	α_{real} - $\alpha_{estimated}$	β_{real} (°) - $\beta_{estimated}$ (°)
		0.12	-0.0083	-14.45
	16	0.27	-0.0056	-7.71
		0.38	-0.0001	6.54
		0.12	-0.0069	-8.60
	38	0.27	-0.0008	-1.92
		0.38	0.0043	4.01
		0.12	-0.0031	-0.39
0.43	77	0.27	0.0020	0.24
		0.38	0.0002	1.51
		0.12	-0.0017	-1.19
	113	0.27	-0.0040	-5.69
		0.38	-0.0005	-0.75
		0.12	-0.0034	-3.99
	176	0.27	-0.0018	-1.31
		0.38	-0.0025	4.54

Also, each α value has been combined with 5 β values (β = 16°, β = 38°, β = 77°, β = 113° and β = 176°) and, last, for each couple (α, β) 3 rotation speeds have been considered (p = 0.12, p = 0.27 and p = 0.38).

According to the results found in Tables 4-6, regarding the crack depth estimation, it can be considered the correlation between calculated and real data is very good, since in all cases the absolute residuals are less than 0.01. In the case of β parameter, eccentricity angle, the differences between both values are always less than 15°.

4.1.3 Robustness of the proposed methodology

The final aim of the explained methodology is to apply it to real systems. In order to simulate actual measurements of a rotor, sensitivity to the errors has also been studied. So that, random noise has been generated and it has been added to the Jeffcott rotor model responses (specifically p, P_1 and P_2 inputs) with 1%, 2% and 5% of its values as random noise.

The sensitivity analysis has been calculated for some α and β values randomly chosen from the previous section. Tables 7-8 show the obtained residuals in this analysis for some α and β, respectively.

Tables 7-8 show the results corresponding to the residuals obtained when different levels of noise are considered in the input data. As an example, 3 combinations of crack depths and angles of eccentricity are shown at different rotating speeds. The residuals are small, for any level of noise, in the case of α, so we can conclude that the procedure is able to be used to identify the crack depth with success. On the other hand, the residuals obtained are larger for the estimation of the angle of eccentricity (β). Nevertheless, the main challenge of the procedure is the identification of the crack, being the determination of the angle position of the eccentricity a collateral result of the research work.

Table 7 α residuals obtained from the sensitivity analysis

	Noise		1%	2%	5%
α = 0.18	β = 38°	p = 0.12	0.0015	0.0007	-0.0033
α = 0.31	β = 16°	p = 0.38	0.0029	-0.0097	0.0075
α = 0.43	β = 113°	p = 0.27	0.0011	0.0062	-0.0047

Table 8 β residuals (°) obtained from the sensitivity analysis

	Noise		1%	2%	5%
α = 0.18	β = 38°	p = 0.12	6.73	-12.07	10.84
α = 0.31	β = 16°	p = 0.38	6.83	-28.75	15.73
α = 0.43	β = 113°	p = 0.27	-1.34	3.85	-9.15

5. Conclusions

In this work, a methodology for cracked rotors diagnosis is presented. It is based on Artificial Neural Networks and the data offered by the frequency spectrum of the rotating damaged shaft. It consists in unbalancing the system in a controlled way, namely, a known eccentric mass is placed at an established distance from the center of the disc. Then, the frequency spectrum of the rotor displacements is obtained. Based on the amplitudes of the first and second frequencies peaks, that can be found in the spectrum, the proposed ANN algorithm can estimate two unknown parameters, both the crack depth (α) and the angle between the unbalance force and the perpendicular direction to the crack front (β). Besides, the developed method takes into account that it is a non-linear problem, due to the crack breathing mechanism during a shaft rotation.

The methodology verification has been completed with a sensitivity to the errors study, in order to simulate experimental measurements. The obtained results confirm the robustness of the developed method, since the crack depth is estimated with very tiny errors, while the obtained angle of eccentricity residuals is larger. Nevertheless, although β estimation is acceptable in most cases, the main challenge of the procedure is the identification of the crack, being the determination of the angle position of the eccentricity a collateral result of the research work. In addition, the method is more accuracy in the case of low and medium rotation speeds, different from resonance speeds.

In summary, the proposed methodology, that could be applicable to any rotating machine, would allow detecting and identifying the crack in unbalanced cracked rotors in order to establish adequate maintenance plans.

Acknowledgments

The authors would like to thank the Spanish *Ministerio de Economía y Competitividad* for the support for this work through the projects DPI2009-13264 and DPI2013-45406-P.

References

Abarici, H. and Bilgin, O. (2009), "Neural network classification and diagnosis of broken rotor bar faults by means of short time Fourier transform", *Proceedings of the International MultiConference of Engineers and Computer Scientists*, Hong Kong, October.

Adewusi, S.A. and Al-Bedoor, B.O. (2002), "Detection of propagating cracks in rotors using neural networks", *Proceedings of the Pressure Vessels and Piping Conference*, Vancouver, Canada, August.

Al-Shudeifat, M.A. and Butcher, E.A. (2010), "On the modeling of open and breathing cracks of a cracked rotor system", *Proceedings of the Special Conference on Mechanical Vibration and Noise*, Montreal, Canada, August.

Al-Shudeifat, M.A. and Butcher, E.A. (2011), "New breathing functions for the transverse breathing crack of the cracked rotor systems: approach for critical and subcritical harmonic analysis", *J. Sound Vibr.*, **330**, 526-544. https://doi.org/10.1016/j.jsv.2010.08.022

Ansari, A.I., Chauhan, S.J. and Khaire, P. (2017), "Effect of crack on natural frequency in rotor system", *AIP Conference Proceedings*, **1859**, 020101. https://doi.org/10.1063/1.4990254

Babu, T.R., Srikanth, S. and Sekhar, A.S. (2008), "Hilbert Huang transform for detection and monitoring of crack in a transient rotor", *Mech. Syst. Signal Pr.*, **22**, 905-914. https://doi.org/10.1016/j.ymssp.2007.10.010

Cavalini, A.A. Jr., Sanches, L., Bachschmid, N. and Steffen, V. Jr. (2016), "Crack identification for rotating machines based on a nonlinear approach", *Mech. Syst. Signal Pr.*, **79**, 72-85. https://doi.org/10.1016/j.ymssp.2016.02.041

Chan, R.K.C. and Lai, T.C. (1995), "Digital simulation of a rotating shaft with a transverse crack", *Appl. Math. Model*, **19**, 411-420. https://doi.org/10.1016/0307-904X(95)00014-B

Chandra, N.H. and Sekhar, A.S. (2016), "Fault detection in rotor bearing systems using time frequency techniques", *Mech. Syst. Signal Pr.*, **72-73**, 105-133. https://doi.org/10.1016/j.ymssp.2015.11.013

Civera, M., Zanotti Fragonara, L. and Surace, C. (2017), "A novel approach to damage localization based on bispectral analysis and neural network", *Smart Struct. Syst., Int. J.*, **20**(6), 669-682. https://doi.org/10.12989/sss.2017.20.6.669

Darpe, A.K., Gupta, K. and Chawla, A. (2004), "Transient response and breathing behaviour of a cracked Jeffcott Rotor", *J. Sound Vib.*, **272**, 207-243. https://doi.org/10.1016/S0022-460X(03)00327-4

Dimarogonas, A.D. (1992), "A brief story of rotor dynamics", *Proceedings of the International Conference on Rotating Machine Dynamics*, Venice, Italy, April.

Dong, G., Chen, J. and Zou, J. (2004), "Parameter identification of a rotor with an open crack", *Eur. J. Mech. A-Solid*, **23**, 325-333. https://doi.org/10.1016/j.euromechsol.2003.11.003

Dong, H.B., Chen, X.F., Li, B. Qi, K.Y. and He, Z.J. (2009), "Rotor crack detection based on high-precision modal parameter identification method and wavelet finite element model", *Mech. Syst. Signal Pr.*, **23**, 869-883. https://doi.org/10.1016/j.ymssp.2008.08.003

El Arem, S. and Zid, M.B. (2017), "On a systematic approach for cracked rotating shaft study: breathing mechanism, dynamics and instability", *Nonlinear Dyn.*, **88**, 2123-2138. https://doi.org/10.1007/s11071-017-3367-7

Gasch, R. (2008), "Dynamic behaviour of the Laval rotor with a transverse crack", *Mech. Syst. Signal Pr.*, **22**, 790-804. https://doi.org/10.1016/j.ymssp.2007.11.023

Genta, G. (2005), Dynamics of rotating systems, Springer, New York, NY, USA.

Gómez-Mancilla, J., Sinou, J.J., Nosov, V.R., Thouverez, F. and

Zambrano, A.R. (2004), "The influence of crack-imbalance orientation and orbital evolution for an extended cracked Jeffcott Rotor", *Comptes Rendus Mécanique*, **332**(12), 955-962. https://doi.org/10.1016/j.crme.2004.09.007

Guo, C., Al-Shudeifat, M.A., Yan J., Bergman, L.A., McFarland, D.M. and Butcher, E.A. (2013), "Application of empirical mode decomposition to a Jeffcott rotor with a breathing crack", *J. Sound Vibr.*, **332**, 3881-3892. https://doi.org/10.1016/j.jsv.2013.02.031

Guo, C., Yan, J. and Yang, W. (2017), "Crack detection for a Jeffcott Rotor with a transverse crack: An experimental investigation", *Mech. Syst. Signal Pr.*, **83**, 260-271. https://doi.org/10.1016/j.ymssp.2016.06.011

Hakim, S.J.S. and Abdul Razak, H. (2014), "Modal parameters based structural damage detection using artificial neural networks - A review", *Smart Struct. Syst., Int. J.*, **14**(2), 159-189. http://dx.doi.org/10.12989/sss.2014.14.2.159

Haykin, S. (1998), *Neural Networks*: *A Comprehensive Foundation*, (2nd edition), Pearson Education Inc., Singapore.

Jun, O.S., Eun, H.J., Earmme, Y.Y. and Lee, C.W. (1992), "Modelling and vibration analysis of a simple rotor with breathing crack", *J. Sound Vibr.*, **155**, 273-290. https://doi.org/10.1016/0022-460X(92)90511-U

Kekan, A.H. and Kumar, B.R. (2019), "Crack depth and crack location identification using artificial neural network", *Int. J. Mech. Product. Eng. Res. Develop.*, **9**(2), 699-708. https://doi.org/10.1016/0022-460X(92)90511-U

Kumar, C. and Rastogi, V. (2009), "A brief review on dynamics of a cracked rotor", *Int. J. Rotating Mach.*, 750108. http://dx.doi.org/10.1155/2009/758108.

Kumar, V.S., Nagaraju, C.H. and Venkatrao, K. (2018), "Modeling and characterization of crack depth on rotor bearing using artificial neural networks", *Int. J. Mech. Eng. Technol.*, **9**(3), 813-827.

Liang, Y., Feng, Q., Li, H. and Jiang, J. (2019), "Damage detection of shear buildings using frequency-change-ratio and model updating algorithm", *Smart Struct. Syst., Int. J.*, **23**(2), 107-122. https://doi.org/10.12989/sss.2019.23.2.107

Liu, S.W., Huang, J.H., Sung, J.C. and Lee, C.C. (2002), "Detection of cracks using neural networks and computational mechanics", *Comput. Methods Appl. Mech. Eng.*, **191**, 2831-2845. https://doi.org/10.1016/S0045-7825(02)00221-9

Matlab (2002), *MATLAB™*, Neural network toolbox users guide.

Mobarak, H.M., Wu, H., Spagnol, J.P. and Xiao, K. (2002), "New crack breathing mechanism under the influence of unbalance force", *Arch. Appl. Mech.*, **88**, 341-372. https://doi.org/10.1007/s00419-017-1312-3

Mogal, S.P. and Lalwani, D.I. (2014), "A brief review on fault diagnosis of rotating machineries", *Appl. Mech. Mater.*, **541**, 635-640. https://doi.org/10.4028/www.scientific.net/AMM.541-542.635

Mohammed, A.A., Neilsom, R.D., Deans, W.F. and MacConnell, P. (2014), "Crack detection in a rotating shaft using artificial neural networks and PSD characterisation", *Meccanica*, **49**, 255-266. https://doi.org/10.1007/s11012-013-9790-z

Muller, P.C., Bajkowski, J. and Soffker, D. (1994), "Chaotic motions and fault detection in a cracked rotor", *Nonlinear Dyn.*, **5**, 233-254. https://doi.org/10.1007/BF00045678

Muñoz-Abella, B., Rubio, L. and Rubio, P. (2015), "Stress intensity factor estimation for unbalanced rotating cracked shafts by artificial neural networks", *Fatigue Fract. Eng. Mater. Struct.*, **38**(3), 352-367. https://doi.org/10.1111/ffe.12237

Nelson, H.D. (1998), "Rotordynamic modeling and analysis procedures: a review", *JSME Int. J. C-Mech. Sy.*, **41**(1), 1-12. https://doi.org/10.1299/jsmec.41.1

Papadopoulos, C.A. (2004), "Some comments on the calculation of the local flexibility of cracked shafts", *J. Sound Vib.*, **278**, 1205-1211. https://doi.org/10.1016/j.jsv.2003.12.023

Papadopoulos, C.A. (2008), "The strain energy release approach for modeling cracks in rotors: A state of the art review", *Mech. Syst. Signal Pr.*, **22**, 763-789. https://doi.org/10.1016/j.ymssp.2007.11.009

Papadopoulos, C.A. and Dimarogonas, A.D. (1987), "Coupled longitudinal and bending vibrations of a rotating shaft with an open crack", *J. Sound Vibr.*, **117**, 81-93. https://doi.org/10.1016/0022-460X(87)90437-8

Park, S., Jeong, H., Min, H. Lee, H. and Lee, S. (2018), "Wavelet-like convolutional neural network structure for time-series data classification", *Smart Struct. Syst., Int. J.*, **22**(2), 175-183. https://doi.org/10.12989/sss.2018.22.2.175

Patel, T.H. and Darpe, A. (2008), "Influence of crack breathing model on nonlinear dynamics of a cracked rotor", *J. Sound Vib.*, **311**, 953-972. https://doi.org/10.1016/j.jsv.2007.09.033

Pu, Y., Chen, J., Zou, J. and Zhong, P. (2002), "Quasi-periodic vibration of cracked rotor on flexible bearings", *J. Sound Vib.*, **251**, 875-890. https://doi.org/10.1006/jsvi.2001.4018

Qin, W.Y., Meng, G. and Zhang, T. (2003), "The swing vibration, transverse oscillation of cracked rotor and the intermittence chaos", *J. Sound Vib.*, **259**, 571-583. https://doi.org/10.1006/jsvi.2002.5095

Rubio, L. and Fernández Sáez, J. (2012), "A new efficient procedure to solve nonlinear dynamics of a cracked rotor", *Nonlinear Dyn.*, **70**, 1731-1745. https://doi.org/10.1007/s11071-012-0569-x

Rubio, P., Muñoz-Abella, B. and Rubio, L. (2018), "Neural approach to estimate the stress intensity factor of semi-elliptical cracks in rotating cracked shafts in bending", *Fatigue Fract. Eng. Mater. Struct.*, **41**(3), 539-550. https://doi.org/10.1111/ffe.12717

Sabnavis, G., Kirk, R.G., Kasarda, M. and Quinn, D. (2004), "Cracked shaft detection and diagnostics: a literature review", *Shock Vib. Digest*, **36**(4), 287-296. https://doi.org/10.1177/0583102404045439

Sampaio, D.L. and Nicoletti, R. (2016), "Detection of cracks in shafts with the approximated entropy algorithm", *Mech. Syst. Signal Pr.*, **72-73**, 286-302. https://doi.org/10.1016/j.ymssp.2015.10.026

Sekhar, A.S. (2004), "Model-based identification of two cracks in a rotor system", *Mech. Syst. Signal Pr.*, **18**, 977-983. https://doi.org/10.1016/S0888-3270(03)00041-4

Shanker, M., Hu, M.Y. and Hung, M.S. (1996), "Effect of Data Standardization of Neural Network Training", *Omega*, **24**(4), 385-397. https://doi.org/10.1016/0305-0483(96)00010-2

Sinou, J.J. (2008), "Detection of cracks in rotor based on the 2X and 3X super-harmonic frequency components and the crack-unbalance interaction", *Commun. Nonlinear Sci. Numer. Simul.*, **13**, 2024-2040. https://doi.org/ 10.1016/j.cnsns.2007.04.008

Sinou, J.J. and Lees, A.W. (2005), "The influence of cracks in rotating shafts", *J. Sound Vib.*, **285**, 1015-1037. https://doi.org/10.1016/j.jsv.2004.09.008

Sinou, J.J. and Lees, A.W. (2007), "A non-linear study of a cracked rotor", *Eur. J. Mech. A-Solid*, **26**(1), 152-170. https://doi.org/10.1016/j.euromechsol.2006.04.002

Söffker, D., Wei, C., Wolff, S. and Saadawia, M.S. (2016), "Detection of rotor cracks: comparison of an old model-based approach with a new signal-based approach", *Nonlinear Dyn.*, **83**, 1153-1170. https://doi.org/10.1007/s11071-015-2394-5

Spagnol, J.P., Wu, H. and Yang, C. (2018), "Vibration Analysis of a Cracked Rotor with an Unbalance Influenced Breathing Mechanism", *Int. J. Mech. Eng. Robot.*, **7**(1), 22-29. https://doi.org/10.18178/ijmerr.7.1.22-29

Varney, P. and Green, I. (2013), "Rotordynamic crack diagnosis: Distinguishing crack depth and location", *J. Eng. Gas Turbine Power*, **135**(11), 112101. https://doi.org/10.1115/1.4025039

Walker, R., Perinpanayagam, S. and Jennions, I.K. (2013), "Rotordynamic faults: recent advances in diagnosis and prognosis", *Int. J. Rotating Mach.*, 856865. hrttp://dx.doi.org/10.1155/2013/856865

Wang, H. and Chen, P. (2009), "Intelligent diagnosis method for a centrifugal pump using features of vibration signals", *Neural Comput. Appl.*, **18**, 397-405. https://doi.org/10.1007/s00521-008-0192-4

Xiang, J., Zhong, Y., Chen, X. and He, Z. (2008), "Crack detection in a shaft by combination of wavelet-based elements and genetic algorithm", *Int. J. Solids Struct.*, **45**, 4792-4795. https://doi.org/10.1016/j.ijsolstr.2008.04.014

Xu, Y., Chen, D.-M, Zhu, W., Li, G. and Chattopadhyay, A. (2019), "Delamination identification of laminated composite plates using measured mode shapes", *Smart Struct. Syst., Int. J.*, **23**(2), 195-205. https://doi.org/10.12989/sss.2019.23.2.195

Zapico-Valle, J.L., Rodríguez, E., García-Diéguez, M. and Cortizo, J.L. (2014), "Rotor crack identification based on neural networks and modal data", *Meccanica*, **49**, 305-324. https://doi.org/10.1007/s11012-013-9795-7

Zhang, C.L., Li, B. and Yang, Z.B. (2013), "Crack location identification of rotating rotor systems using operating deflection shape data", *Sci. China Tech. Sci.*, **56**, 1723-1732. https://doi.org/10.1007/s11431-013-5243-0

FC